<u>Response to Reviewer #1</u>

We thank the reviewer for their constructive commentary about our work. Comments received about the implementation of the boundary conditions of the domain prompted a review and recalculation of our simulations, resulting in significantly different results. We moved from using elevations as prescribed by TPXO8 to those from a global forward model. For computational cost and time reasons this model was run using the M2 and K1 constituents only, making it necessary to limit the manuscript results to these constituents. Unfortunately this means our discussion of S2 no longer appears in the manuscript, and any suggestions pertaining to this section cannot be addressed.

GENERAL COMMENTS

The present work, is, to my knowledge the first regional study of SLR effect on tides in this area (Australasia), even if global studies already provided indications (e.g. Pickering et al, 2017; Schindelegger et al., 2018). In addition, a well-established model is used, together with published methods of analysis. This make this paper suitable for a potential publication. However, the paper lacks a description of the present-day tidal dynamics. The model validation lacks some elements to be fully convincing. In addition, the comparison of the observed trend and modelled trend rises questions on the SLR value choice. The paper is sometime difficult to read (especially when describing results per areas not indicated in maps). The provided physical explanations of the results deserve to be more strongly supported. Some figures and maps are probably lacking (regarding the text), and deserve to be in an Appendix.

MAJOR REMARKS

1.Site description

The paper lacks description on the tidal dynamics in the study site, making the results more difficult to interpret. A minimum level of description should be provided. Maps of M2, S2, K1 amplitudes (and perhaps phase) would be useful.

The figure showing the bathymetry of the domain has been expanded to include a chart of M2, and a supplemental figure of K1 has also been included. We hope the additional references to this figure in the text and the expanded description of the control simulation in the Results section [page 10, line 4] help the reader to visualise the changes we describe.

2.Model validation

Regarding the validation of the amplitude of M2, S2, K1, statistical information as correlation coefficient and bias would allow to better characterize the model errors, and also to better support the text. In particular, it is stated that the model overestimates K1. An explanation is given. But, looking at Figure 2, I have the impression that S2 is also over-estimated. If this is the case, then the explanation would not be reliable anymore. In addition, there is no physical explanations provided for the sites which are beyond the 2+/- standard deviation and these sites are not identified (we do not know where the model “fails”). Regarding the comparison between the modeled trend and observed trend, I have a concern on the SLR choice. Indeed, I do not understand why using SLR=1m, rather than a more probable value for the last decades. The underlying assumptions (not stated in section 2.4, but stated later on) is that the changes are proportional to SLR. While this has been proved to be true in some locations, this is can be locally not true. The validation of trends deserve more attention, either by checking the proportionality of changes in the [0-1m] or using a more realistic SLR value (or a non-uniform SLR field) for the last decades. As to me Figure 3 and the text is not fully convincing, I strongly recommend to have a closer look on this point. In addition, the validation should also be done for S2 and K1.

This comment contains several threads. Our responses to each of those threads are as follows:

(1) Validation of the M2 and K1 control run and discussion of outliers: we have reworked Section 2.4 [page 8, line 5-10] to explain model-to-data discrepancies beyond the 1-sigma-level (stations Williamstown and Geelong). Correlation coefficients and median absolute differences have been included as additional statistical measures. Note that upon exclusion of the two “outliers”, RMS differences improve significantly w.r.t. the previous version of the manuscript.

(2) Possible overestimation of K1: even though our new Figure 2 contains slight hints of such an overestimation, we have refrained from speculations in this regard.

(3) SLR choice: we tried to redo both our new global and the Australian domain simulations with a few dm of SLR, but obtained suspicious tidal changes, possibly related to numerical artifacts arising in the model at such small values of SLR. Therefore, the validation is still done with the M2/K1 results for 1 m.

(4) Validation of trends for constituents other than M2: we have performed the necessary computations for K1 and show the corresponding figure in the supplement. Finally, we note that alongside SLR, other processes (e.g., ocean warming, thermocline deepening, changes in shoreline position, local anthropogenic influences such as periodic dredging) could have contributed to observed changes in the tides, so a comparison to model values from SLR-only scenarios can't be fully convincing. Figure 3 rather documents partial success in capturing observed tidal variability at a number of stations. Additional formulations pertaining to this issue have been added to the text in Section 2.4.

3.Physical mechanisms

Several times in the paper, the authors provide some explanation on the results (quality or SLR effect) using the words "probably", "presumably". This weakens the paper. As much as possible, the authors should provide more evidence to support their interpretations. As written in the discussion a series of numerical tests could be done to better asses the resonance and frictional effects. I strongly recommend to perform these experiments in the present paper to really support the interpretations. As a more minor remark, the model does not include advection terms. What could be the effect of neglecting this term on the present results? Is there any literature justifying to neglect it for tide modeling?

We have followed the first suggestion and removed many of the conjectures in the original manuscript. With the efforts and textual changes demanded by this revision and the new simulations, we think that more numerical tests fall beyond the scope of our study.
As far as the advection terms are concerned, these can be neglected with little drop in accuracy (as per Egbert et al., 2004), with the added benefit of reducing the computational workload of the model runs. Also, test runs by one of the authors (M. Schindelegger) with another tidal model showed that M2 responses around Australia to a 2 m uniform SLR change by no more than 2 mm between simulations with and without advective terms.

4.Figures

- Maps of M2, S2, K1 amplitudes are lacking.

Maps of M2 and K1 amplitudes are now included alongside the bathymetry and in the supplementary information respectively.

- The text relies on many results, which are not shown (e.g. tide changes of M2, S2, K1 for SLR different that the 1 and 7 m shown in the paper). Such figures would be useful and could be added in Appendix.
The text is now more focused on what is shown in the figures and does no more rely on results for SLR other than 1 and 7 m. Note also that there are only slight variations in the spatial distribution of the tide changes for SLR different to 1 m and 7 m; we have therefore refrained from including these results in the appendix (or supplement).

- The text describes the results using the names of many locations. A map indicating all this locations is needed (a reader not knowing Australia will have to make a big effort to follow the description).

Figure 1 now includes markers showing the location of discussed topographical features, and labels naming specific bodies of water.

- In the text, there are also some comments on tide changes south of Australia. Some figures to support this text would be useful, in appendix for instance.

Figure 5, showing the south coast of Australia, has been included in the manuscript.

"ON-LINE" REMARKS

- P1-Line 14: sentence "At sea level . . .." is a bit strange. Why insisting on well-suited farming?

The wording has been altered to a more general description of the suitability of coasts for human settlement, rather than a specific example. Reference to "At sea level" has been changed to "Coastal areas"

- P1-Line 16: provide a number together with the 85% would be more meaningful

A population number has been included alongside the population percentage: "85% of the population of Australia (approximately 19.9 million people; ABS, 2016)"

P2-Line 12: Pickering et al., 2012 -> Pickering et al., 2017

Modified as suggested by the reviewer

- P5-Line 7: why focusing on M2, S2, K1? Some explanations should be provided. Perhaps they are the dominant tidal components but it should be said (relying on reference or map?).

Our new simulations focus on only M2 and K1 which are the dominant semi-diurnal and diurnal constituents in the domain which is now referenced to in Section 2.1. We have included Figures showing the control M2 and K1 amplitudes.

- P5-Line 25: as the authors made the computation under non-uniform SLR, this would be useful/interesting to add in appendix the tide changes induced considering the non-uniform SLR.
A figure showing the difference in result between uniform and non-uniform SLR has been included in the supplement, discussing our investigation into using spatially non-uniform SLR patterns

- P7-Line 3-5: "These statistics . . .". The authors do not provide enough evidence that this is the spatial resolution that could explain the discrepancies. More detailed analysis is required to support this hypothesis.
New analysis shows good agreement with all stations apart from Williamstown and Geelong, which are unique in that they are confined within Port Phillip Bay. This narrow headlands which confine this bay are too small a feature to be captured by the model resolution. How this area is treated in the model is now discussed.

- P8-Line 2-3: remind that this was for a given range of SLR in "Idier et al. (2017)", and also for a given area (NW European shelf).

Modified as suggested by the reviewer.

- P14-Line 14: "SLR has a broadly linear effect on the amplitude of the semi-diurnal constituents out on the open shelf, but causes increasingly large semi-diurnal amplitudes, and correspondingly high tidal dissipations, within embayments such as King Sound". I did not see "the linear" effect on the figures. Looking at Figure 4, 8 and 9, notable differences can be observed offshore between the two SLR scenarios. This point deserves more explanation, and probably some kind of maps showing proportionality coefficients of tide changes with SLR, as for instance in (Pickering et al., 2017) or in (Idier et al., 2017).

With the new simulations we have performed this point of ours is no longer valid and has been removed from the text.

- P15-Line 16: why was it computationally necessary to cross the shelf? Are the authors referring here to computational time? If yes, then it should be stated more clearly and computation time should be provided. In addition, one simulation on a larger domain for a very large SLR would allow estimating the effect of the assumption that tidal components are unchanged on this north boundary.

This point is has been addressed by the new simulations and the formulations in question have been removed from the text.

<u>Response to Reviewer #2</u>

I recommend major revisions for this manuscript. The topic, tidal changes around the Australasia region, is interesting. The study adds to the literature on projected tidal changes in response to sea level rise with a high-resolution model of the Australasia region. As far as I can tell, the study has been done competently. The writing is generally clear, with some exceptions noted below. The main cause for my concern is that, as far as I can tell, the authors have used TPXO boundary conditions throughout their study. The TPXO boundary conditions are from the present day, meaning that the tides along the boundaries are not responding to changes in sea level rise. The fact that the regional model has some skill in simulating observed tidal changes suggests that maybe this is OK. On the other hand, the authors have a high-resolution forward global tide model available to them; why didn't they use it here? Global tide models would respond to the changes in sea level, thus providing more natural boundary conditions. Would the computational expense be too great? If so, say so, and provide some evidence for that, or at least make it more clear that we shouldn't worry too much about this. If it is feasible, I suggest that the authors use the global tide models to complement at least some of the simulations with TPXO boundary conditions.

We thank the reviewer for their constructive commentary about our work. Comments received about the implementation of the boundary conditions of the domain prompted a review and recalculation of our simulations, resulting in significantly different results. We moved from using elevations as prescribed by TPXO8 to those from a global forward model. For computational cost and time reasons this model was run using the M2 and K1 constituents only, making it necessary to limit the manuscript results to these constituents. Unfortunately this means our discussion of S2 no longer appears in the manuscript, and any suggestions pertaining to this section cannot be addressed.

Other important suggestions:
1) Where does the SAL term come from in this regional model? This is an important detail, that should be described.

The SAL term is derived from TPXO8 data. This has been clarified in Section 2.1.; "The model solves equations 1–2 using forcing from the astronomic tide generating potential only … and the SAL term is derived from TPXO8"

2) Page 5, lines 20-29: The 1 and 7 meter sea level rise values are justified, but the 3, 5, 15, and 20 meter sea level rise values are not explicitly justified. 3 and 5 lies between 1 and 7, the latter being an "extreme value" so I'm guessing that might justify the 3 and 5 meter values; but again, it would be nicer if the authors themselves made an explicit justification. And the 15 and 20 meter values are not justified at all.

Our new simulations have used 1, 3, 5, 7 and 12 m SLR. The 3 and 5 m values follow from Wilmes et al., 2017, (as the global mean sea level increase from the collapse of just the marine sectors of the West Antarctic Ice Sheet and the total collapse of the WAIS respectively), which is now stated in Section 2.3. Whilst 12 m may not be physically justified, it allows us to see how trends may continue; this has been stated in the text.

3) It seems to me that readers would take more away from the discussion of Figure 1 if the tide trends were compared to the MSL trends/increases. Are the tidal trends comparable? Other papers e.g. Jay 2009 have commented on this-in some regions, the tidal and MSL trends are comparable. This helps the readers to envision the societal significance of the tidal trends. I suggest adding some commentary on this for the Australasia region.

This is a good point. A brief discussion of this has been added to the introduction.

Minor comments:
Page 6 line 4-suggest “With a few exceptions, record lengths are short, but all . . .”
Page 6 line 20-suggest “. . .constituent amplitudes. . .” in place of “. . .constituents amplitudes. . .”

The above modifications suggested by the reviewer have been made where possible (some sentences referred to no longer exist in the manuscript)

Page 7, line 29-can the stated greater impact of sea level rise on tides be justified with a citation or some other source of information?

This comment was written with a current review paper by Haigh et al. (submitted to Reviews of Geophysics) in mind. We could cite is as ”gray literature” here but rather prefer to wait, see how this reference paper evolves, and include it later during the editing process.

Page 9, line 8-suggest “amplification of the tide” (insert “the”)
Figure 6 caption – “W mˆ2” i.e. should instead be “W mˆ-2”
Page 12, line 12-suggest “. . .Arafura Sea. The changes in S2 amplitude appear similar to the changes in M2 amplitude, including. . .”
Page 13, lines 3-5-suggest “Because S2 is a tidal constituent, its response. . .”
Paige 13, line 6-suggest “In contrast to the M2 behavior, above 7 m. . .”
Page 13, line 10-the phrase beginning with “yet” sounds odd to me. The M2 and S2 dissipation patterns are similar but the M2 values are much larger. That is not surprising, so inserting a phrase beginning with “yet” seems out-of-place, to me at least. Minor point, but I suggest omitting this phrase.
Page 13, line 13-suggest “The K1 changes are relatively limited compared to the changes in the semi-diurnal constituents examined here.”
Page 14, line 6-this sentence reads awkwardly. Please improve the grammar.
Page 14, line 17-I believe that the word after “SLR” should be “on” not “of”
Page 15, lines 10-11-“impact to” should be “impact on”
Page 15, line 13-“model concerns” is an odd-sounding phrase
Page 15, line 15-“changes to changes”. Is this what you want to say?

The above modifications suggested by the reviewer have been made where possible (some sentences referred to no longer exist in the manuscript)

<u>**Response to the Editor’s comments**</u>

We thank the editor for their constructive commentary about our work. Comments received about the implementation of the boundary conditions of the domain prompted a review and recalculation of our simulations, resulting in significantly different results. We moved from using elevations as prescribed by TPXO8 to those from a global forward model. For computational cost and time reasons this model was run using the M2 and K1 constituents only, making it necessary to limit the manuscript results to these constituents. Unfortunately this means our discussion of S2 no longer appears in the manuscript, and any suggestions pertaining to this section cannot be addressed.

A first is the word Australasia in the title. Australasia means Australia, New Zealand and the west Pacific islands and (maybe) Papua New Guinea. But there is no discussion of New Zealand tides in the text, so at first I thought Australasia should be replaced by Australia. But then many of the figures even cut off the southern part of Australia. Why was that? So I think the title might be revisited.

The title has been revised in line with your comment. The previous focus on the north of Australia was because that was where most of the notable changes to amplitude within the domain occurred. As of the new simulations undertaken, a new figure showing the south has been included.

page 1, line 5 and 8 - there are mentions in the abstract and text of places that can be unfamiliar and so need qualifying e.g. on line 5 this should be Arafura Sea (between Australia and Papua New Guinea). On line 8 Papua should be Papua New Guinea I guess (Papua is a province of Indonesia which I think is not is what is meant). Some of these places are later pointed out in Figure 1 but the reader will not know them at this point.

The abstract has been rewritten with, hopefully, more immediately recognisable descriptions of locations.

22 - I don’t understand why Woodworth (2017) is given here. It is not relevant to the sentence.

This was a mistaken placement of the reference, now removed

page 2, line 1 - the main peaks in extremes in most parts of the ocean, where there is a semidiurnal tide, are every 4.4 years or so from the perigean cycles in the moon’s orbit. You get peaks in extremes every 18.6 years where there are diurnal tides. You could references Haigh (JGR, 2011) for example or Pugh and Woodworth (2014) or Merrifield et al. (JGR, 2013).
10 - again I don’t see why the Mawdsley reference is relevant to this sentence.
13-15 - you could reference the AR5 somewhere here.
23 - phenomena –> phenomenon

The above spelling and reference suggestions have been implemented

24 - again, who knows where the Sahul shelf is?

Potentially confusing place names have been removed, and the locations discussed in the paper are now all found in Figure 1.

26 - dissipation on a par with the Yellow Sea ..

Changed to “...dissipation comparable to that of the Yellow Sea...”

page 5, eqs. 6 and 7 - these need reformatting
23 ’ ’Additional runs’. I think a few extra words are needed to clarify that these additional runs were not used.

The Section 2.3 has been reformulated to describe the new simulations performed.

page 6, Figure 2 - ok for amplitude. Is phase lag agreement worth showing?

Median phase differences have been calculated and describe in the text [page 8, line 15]

20 - reword ’A comparison of the amplitudes of the constituents calculated ...’

Reworded to “A regression of the constituent amplitudes calculated”

page 7, line 18 - I can see from the figure that the signs are often in agreement, I can’t see the ’reproduces much of the in situ variability’. Needs explaining better.
page 8, line 3 - surely standard deviations should be standard errors?
.... annual tidal estimates of M2. Stations with insignificant measured phase …

Section rewritten to account for above comments

section 3 - this seems to me to need a couple of introduction sentences to say that you will here in this section be testing SLR of 1,3,7 m for the modelling.
page 9, 13 - I don’t see how the reader can relate to 10m change which is not shown, so add (not shown) to make it clear.

Section has been rewritten to discuss the updated simulation.

page 10, in Fig 5 caption and the y-annotation ’phase’ should be ’phase lag’ and it is Greenwich phase lag presumably.

Caption and Figure altered

line 2 - I think this should read:
.. movement of a virtual amphidromic point (an amphidrome over land) (see Fig. 5) ..
to become real (i.e. amphidrome over the ocean) …

Modified as suggested by comment

page 11, line 1 of Figure 6 caption - .. model domain in the control run. You should make clear which way the difference works.

The way the difference works is now explicitly stated in the figure caption “(FL - Control)”

Figure 7 - does the 200m refer to the control run bathymetry?

Yes, this has now been made explicit in the figure caption.

second sentence caption - I don’t think is necessary.

Second sentence in caption has been removed

line 5 - why south coast chopped off?

This was to highlight some of the more complex structure in the dissipation changes. The figure now shows the full domain.

page 12, 1 and 2 - have JBG and VDG acronyms been defined?

The acronyms have been deemed unnecessary and removed.

13 - Eighty-Mile Beach

Sentence has been removed

page 13, Figure 9 - you have FL-cntl and FL-NFL so it might help to have a third column of maps for NFL-cntl so the reader did not have to do mental arithmetic.

The figures originally showed FL-Ctrl beside NFL-Ctrl, however the differences were very difficult to tell by eye – hence why we show NFL-FL instead, which more easily presents the difference. The trade-off is the mental arithmetic, hopefully aiding by the text. I believe a third column would limit the ability of the figures to show some of the smaller details.

line 13 - docile is an odd word. Just say K1 has a small amplitude (< ?? cm)
page 14, 4 - Figure 9c must be 9d
23 - reduce
page 15, 11 - in the amplitude
14-16 - I don’t understand this sentence but anyway ’changes to changes’ needs rewording.

Modified as suggested

The impact of sea-level rise on tidal characteristics around Australia

Alexander Harker[1,2], J. A. Mattias Green[2], Michael Schindelegger[1], and Sophie-Berenice Wilmes[2]

[1]Institute of Geodesy and Geoinformation, University of Bonn, Bonn, Germany
[2]School of Ocean Sciences, Bangor University, Menai Bridge, United Kingdom

Correspondence: Alexander Harker (harker@igg.uni-bonn.de)

Abstract. An established tidal model, validated for present-day conditions, is used to investigate the effect of large levels of sea-level rise (SLR) on tidal characteristics around Australasia. SLR is implemented through a uniform depth increase across the model domain, with a comparison between the implementation of coastal defences or allowing low-lying land to flood. The complex spatial response of the semi-diurnal M_2 constituent does not appear to be linear with the imposed SLR. The most predominant features of this response are the generation of new amphidromic systems within the Gulf of Carpentaria, and large amplitude changes in the Arafura Sea, to the north of Australia, and within embayments along Australia's north-west coast. Dissipation from M_2 notably decreases along north-west Australia, but is enhanced around New Zealand and the island chains to the north. The diurnal constituent, K_1, is found to decrease in amplitude in the Gulf of Carpentaria when flooding is allowed. Coastal flooding has a profound impact on the response of tidal amplitudes to SLR by creating local regions of increased tidal dissipation and altering the coastal topography. Our results also highlight the necessity for regional models to use correct open boundary conditions reflecting the global tidal changes in response to SLR.

1 Introduction

Fluctuations in sea-level at both short and long time scales have had, and will have, a significant influence upon societies in proximity of the coast. Coastal areas are attractive locations for human populations to settle for multiple reasons; the land is often flat and well-suited for agriculture and urban development, whilst coastal waters can be used for transport, trade, and as a source of food. Being a large island nation, 85% of the population of Australia (approximately 19.9 million people; ABS, 2016) live within 50 kilometers of the ocean, and the recreation and tourism industries located along the coast are a key part of Australia's economy (Watson, 2011). As such, Australia is particularly sensitive to both short term fluctuations in sea level (e.g. tidal and meteorological effects) and long term changes in mean sea level (MSL). Tidal changes in sea level are a major influencing factor on coastal morphology, navigation and ecology (Allen et al., 1980; Stumpf and Haines, 1998), and the combination of extreme peaks in tidal amplitude (associated with long period lunar cycles, Pugh and Woodworth, 2014) with storm surges (associated with severe weather events) can be a key component of unanticipated extreme water levels (Haigh et al., 2011; Pugh and Woodworth, 2014; Muis et al., 2016). With sea levels around Australia forecast to rise by up to 0.7 m by the end of the century (McInnes et al., 2015; Zhang et al., 2017), understanding how tidal ranges are expected to vary with changing MSL is crucial for determining the potential implications for urban planning and coastal protection strategies in low-lying areas.

As the dynamical response of the oceans to gravitational forcing, tides are sensitive to a variety of parameters, including water depth and coastal topography. Such changes in bathymetry may have an impact on the speed at which the tide propagates and the dissipation of tidal energy, and it may change the resonant properties of an ocean basin. As an extreme example, during the Last Glacial Maximum (when sea level was approximately 120 m lower than present day) the tidal amplitude of the M_2 constituent in the North Atlantic was greater by a factor of two or more because of amplified tidal resonances there (Egbert et al., 2004; Wilmes and Green, 2014). Consequently, understanding the ocean tides' response to changing sea level has been a subject of recent research, at both regional (Greenberg et al., 2012; Pelling et al., 2013; Pelling and Green, 2013; Carless et al., 2016) and global scales (Müller et al., 2011; Pickering et al., 2017; Wilmes et al., 2017; Schindelegger et al., 2018).

Current estimates of the global average change in sea level over the last century suggest a rise of between 1.2–1.7$\mathrm{mm\ yr^{-1}}$ (Church et al., 2013; Hay et al., 2015; Dangendorf et al., 2017; IPCC, 2013). However, significant inter-annual and decadal-scale fluctuations have occurred during this period, for example over the period 1993–2009, global sea-level rise (SLR) has been estimated at 3.2 $\mathrm{mm\ yr^{-1}}$ (Church and White, 2011; IPCC, 2013). Studies suggest that global sea level may rise by up to 1 m by the end of the 21st century, and by up to 3.5 m by the end of the 22nd century (Vellinga et al., 2009; DeConto and Pollard, 2016). However, sea-level change is neither temporally nor spatially uniform as a multitude of physical processes contribute to regional variations (Cazenave and Llovel, 2010; Slangen et al., 2012). Part of this signal is attributed to increasing ocean heat content causing thermal expansion of the water column, but most of the rise and acceleration in sea level is due to enhanced mass input from glaciers and ice sheets (Church et al., 2013). The effect of vertical land motion, specifically Glacial Isostatic Adjustment (GIA), should also come under consideration; however around the Australian coastline the effect is small (White et al., 2014). Additionally, trends in the amplitude of the M_2 constituent around Australia are as much as 80% of the magnitude of the trend seen in global MSL (Woodworth, 2010), thus the impact of changing tides upon regional variations in sea-level should not be underestimated.

Here, we expand previous tides and SLR investigations to the shelf seas surrounding Australia, which have received little attention so far despite the north-west Australian shelf alone being responsible for a large amount of energy dissipation comparable to that of the Yellow sea or the Patagonian shelf (Egbert and Ray, 2001). Here, we study the region's tidal response to a uniform SLR signal, and consider the impact of coastal defences (inundation of land allowed or coastal flood-defenses implemented) on the tidal response. Wide areas of this region experience large tides at present, and areas such as the Gulf of Carpentaria are influenced by tidal resonances (Webb, 2012). It is therefore expected that we will see large differences in the tidal signals with even moderate SLR, as it is known that a (near-) resonant tidal basin is highly sensitive to bathymetric changes (e.g., Green, 2010). In what follows we introduce OTIS, the dedicated tidal modeling software used, and the simulations performed (Sections 2.1–2.3). To ground our considerations of future tides on a firm observational basis, we conduct extensive comparisons to tide gauge data in Section 2.4. Section 3 presents the results, and the paper concludes in the last section with a discussion.

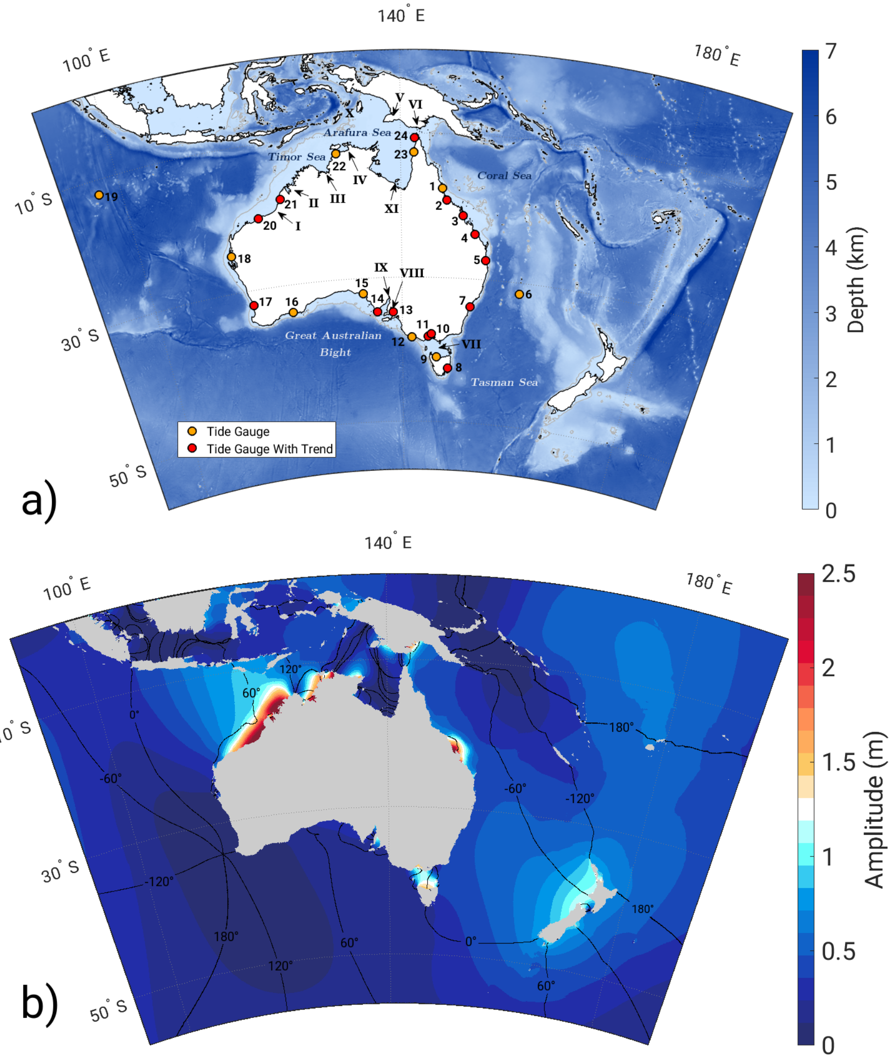

Figure 1. a) Bathymetry of the model domain and tide gauge sites used in the analysis (colored dots): cf Table 1. Locations at which M_2 trends were estimated are shown in red. Regions mentioned in subsequent sections of the paper are marked on the map: I - Eighty Mile Beach, II - King Sound, III - Joseph Bonaparte Gulf, IV - Van Dieman Gulf, V - Yos Sudarso Island, VI - Torres Strait, VII - Bass Strait, VIII - Gulf St. Vincent, IX - Spencer Gulf, X - Arafura Islands, XI - Wellesley Islands. b) Co-tidal chart of the M_2 constituent amplitude for the control simulation. Black lines represent co-phase lines with 60° separation.

Table 1. Start and end dates of the analyzed tide gauge records, including names and running index for identification in Figure 1

Station ID	Name	Time Span	Source
1	Mourilyan Harbour	1986–2014	GESLA
2	Townsville	1980–2014	GESLA
3	Hay Point	1985–2014	UHSLC
4	Gladstone	1982–2014	UHSLC
5	Brisbane	1985–2016	GESLA
6	Lord Howe Island	1992–2014	GESLA
7	Fort Denison	1965–2017	GESLA
8	Spring Bay	1986–2017	GESLA
9	Burnie	1985–2014	GESLA
10	Williamstown	1976–2014	UHSLC
11	Geelong	1976–2014	UHSLC
12	Portland	1982–2014	GESLA
13	Port Adelaide	1976–2014	GESLA
14	Port Lincoln	1967–2014	UHSLC
15	Thevenard	1966–2014	GESLA
16	Esperance	1985–2017	GESLA
17	Fremantle	1970–2014	GESLA
18	Canarvon	1991–2014	GESLA
19	Cocos Islands	1991–2017	GESLA
20	Port Hedland	1985–2014	UHSLC
21	Broome	1989–2017	UHSLC
22	Darwin	1991–2017	GESLA
23	Weipa	1986–2014	GESLA
24	Booby Island	1990–2017	UHSLC

2 Modeling future tides

2.1 Model configuration and control simulation

We use OTIS, the Oregon State University Tidal Inversion Software, to simulate the effects of SLR on the tides around Australia. OTIS is a portable, dedicated, numerical shallow water tidal model which has been used extensively for both global and regional modeling of past, present, and future ocean tides (e.g., Egbert et al., 2004; Pelling and Green, 2013; Wilmes and Green, 2014; Green et al., 2017). It is highly accurate both in the open ocean and in coastal regions (Stammer et al., 2014), and it is computationally efficient. The model solves the linearized shallow-water equations (e.g., Hendershott, 1977) given by

$$\frac{\partial \mathbf{U}}{\partial t} + \mathbf{f} \times \mathbf{U} = -gH\nabla(\zeta - \zeta_{EQ} - \zeta_{SAL}) - \mathbf{F} \tag{1}$$

$$\frac{\partial \zeta}{\partial t} = -\nabla \cdot \mathbf{U} \tag{2}$$

where $\mathbf{U}$ is the depth integrated volume transport, which is calculated as tidal current velocity $\mathbf{u}$ times water depth H. $\mathbf{f}$ is the Coriolis vector, g denotes the gravitational constant, ζ stands for the tidal elevation with respect to the moving seabed, ζ_{SAL} denotes the tidal elevation due to ocean self-attraction and loading (SAL), and ζ_{EQ} is the equilibrium tidal elevation. $\mathbf{F}$ represents energy losses due to bed friction and barotropic-baroclinic conversion at steep topography. The former is represented by the standard quadratic law:

$$\mathbf{F}_B = C_d \mathbf{u}|\mathbf{u}| \tag{3}$$

where $C_d = 0.003$ is a non-dimensional drag coefficient, and $\mathbf{u}$ is the total velocity vector for all the tidal constituents. The parameterization for internal tide drag, $\mathbf{F}_w = C|\mathbf{U}|$, includes a conversion coefficient C, which is defined as (Zaron and Egbert, 2006; Green and Huber, 2013)

$$C(x,y) = \gamma \frac{(\nabla H)^2 N_b \bar{N}}{8\pi^2 \omega} \tag{4}$$

Here, $\gamma = 50$ is a scaling factor, N_b is the buoyancy frequency evaluated at the sea bed, $\bar{N}$ is the vertical average of the buoyancy frequency, and ω is the frequency of the tidal constituent under evaluation. Values of both N_b and $\bar{N}$ follow from the prescription of horizontally uniform stratification $N(z) = N_0 \exp(-z/1300)$, where $N_0 = 5.24 \times 10^{-3}\ \mathrm{s}^{-1}$ has been obtained from a least-squares fit to present-day climatological hydrography (Zaron and Egbert, 2006).

The model solves equations (1)–(2) using forcing from the astronomic tide generating potential only (represented by ζ_{EQ} in Eq. (1)), with the SAL term being derived from TPXO8 (Egbert and Erofeeva, 2002, updated version). An initial spin-up from rest over 7 days is followed by a further 15 days of simulation time, on which harmonic analysis is performed to obtain the tidal elevations and transports. Here, we investigate the two dominating semi-diurnal and diurnal tidal constituents, M_2 and K_1 respectively. The model bathymetry comes from the ETOPO1 dataset (Amante and Eakins, 2009, see Fig. 1 for the present domain), which was averaged to 1/20° horizontal resolution. For the control run with present-day water depths, the domain model heights at the open boundaries were constrained to elevation data from a coarser-resolution global OTIS run, taken from Wilmes et al. (2017). TPXO8 was used to validate the model (alongside tide gauge data at 24 locations); see Section 2.4.

2.2 Dissipation computations

The computation of tidal dissipation rates, D, was done following Egbert and Ray (2001):

$$D = W - \nabla \cdot P \tag{5}$$

Here, W is the work done by the tide-generating force and P is the energy flux given by

$$W = g\rho\langle \mathbf{U}\cdot\nabla(\eta_{SAL}+\eta_{EQ})\rangle \quad (6)$$

$$P = g\langle \eta\mathbf{U}\rangle \quad (7)$$

where the angular brackets mark time-averages over a tidal period.

2.3 Implementing Sea-Level Rise

The model runs are split into two sets. In the first, we allow low-lying grid cells to flood as sea level rises, whereas in the second set we introduce vertical walls at the present-day coastline. Following Pelling et al. (2013), we denote these sets “flood” (FL) and “no flood” (NFL), respectively. A range of SLR scenarios corresponding to predicted global mean sea level increases from large scale ice sheet collapses (Wilmes et al., 2017) are investigated in both sets. This is done via the implementation of a uniform depth increase across the entire domain of 1, 3, 5, 7, and 12 m. Boundary conditions for each of the SLR scenarios are generated from global simulations. The 5, 7, and 12 m SLR NFL runs were taken directly from Wilmes et al. (2017) and the remaining global simulations were carried out following the methodology outlined in Wilmes et al. (2017) but with varying global sea-level changes and allowing for inundation in the FL runs. Additionally, we simulated tidal responses to future changes in water depth extrapolated from geocentric sea-level trend patterns as observed by satellite altimetry (cf. Carless et al., 2016; Schindelegger et al., 2018). While such projections contain not only the actual long-term trend of sea level but also significant (sub-)decadal variability, little difference was found for tidal perturbations with respect to our uniform SLR scenarios (see supporting information). It is also unknown how the magnitude and spatial variation of the trend pattern may change over the period of time required to equate a uniform SLR, especially with the larger scenarios considered here. Hence in the following, the focus is on the uniform SLR scenarios. We choose to show results for the 1 m and 7 m SLR simulations because they best exemplify the changes to tidal characteristics across the domain, and also correspond to a high but probable level for the end of this century and an extreme case in which large levels of ice sheet collapse has occurred, respectively (e.g., Wilmes et al., 2017). The simulations with 12 m of SLR have little physical justification, but they allow us to assess how any tidal trends seen up to 7 m, if they appear, may evolve for even higher levels of SLR.

2.4 Model Validation

For validation of our numerical experiments, time series of hourly sea level data from 24 stations around Australasia were obtained from the Global Extreme Sea Level Analysis Version 2 (GESLA-2; Woodworth et al., 2017) and the University of Hawaii Sea Level Center (UHSLC; Caldwell et al., 2015); see Table 1. With few exceptions, record lengths are short; but all time series span at least 28 years to allow for an appropriate representation of the 18.61-year nodal cycle in lunar tidal constituents (Haigh et al., 2011). Upon removal of years missing more than 25% of hourly observations, a three-tiered least-squares fitting procedure was applied to (i) extract mean M_2 and K_1 tidal constants of amplitude H and phase lag G, (ii) deduce linear trends in H and G for both constituents over the complete time series at each station, and (iii) estimate the corresponding

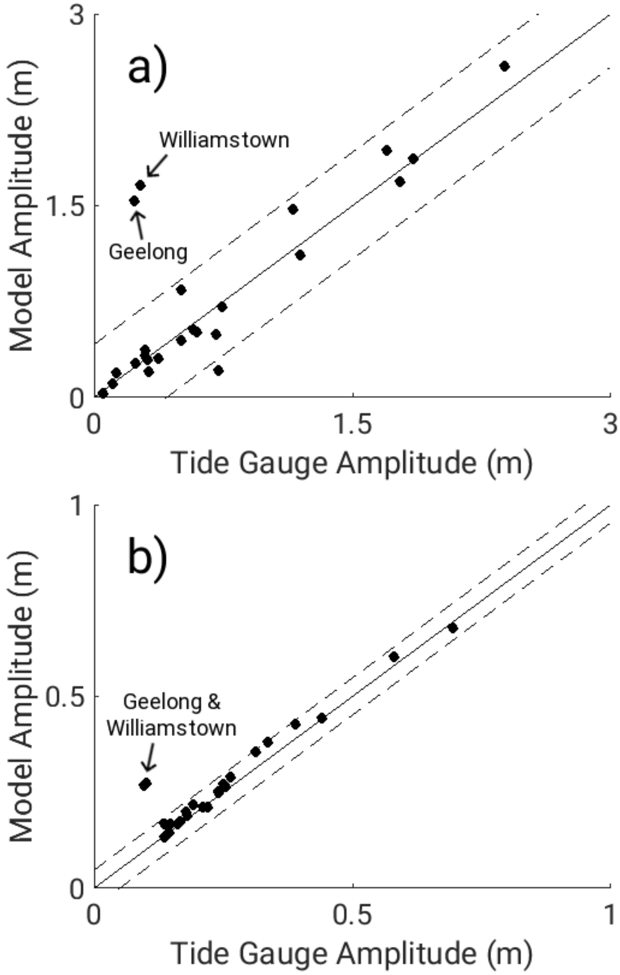

Figure 2. The constituent amplitude at each tide gauge position calculated from GESLA and UHSLC data and the model control simulation for a) M_2 and b) K_1. The solid line marks the zero difference line. The dashed lines mark one standard deviation of the difference.

long-term trend in MSL. 10 out of 24 tide gauge stations yielded statistically insignificant M_2 amplitude trends at the 95% confidence level and were thus excluded from the model trend validation below; see Fig. 1 for a graphical illustration.

The processing protocol, essentially taken from Schindelegger et al. (2018), is based on a separation of tidal and non-tidal residuals from the longer-term MSL component through application of a 4-day moving average with Gaussian weighting. The high-frequency filter residuals obtained were then harmonically analyzed for 68 tidal constituents using the Matlab® UTide software package (Codiga, 2011), with analysis windows either set to the entire time series (step i) or shifted on an annual basis (step ii). In both cases, we configured UTide for standard least squares and a white-noise approach in the computation of confidence intervals. Subsequent regressions of annual M_2 tidal constants were performed with a functional model composed of a linear trend, a lag one-year autocorrelation, AR(1), and sinusoids to account for nodal modulations. Trends in MSL were likewise determined through regression under AR(1) assumptions, upon a priori reduction of the influence of the 18.61-year equilibrium tide.

A regression of the constituent amplitudes calculated from the OTIS control simulation for the present-day bathymetry against the M_2 and K_1 amplitudes from harmonic analysis of the tide gauge data (Fig. 2) reveals that the model performs well at all sample sites except at stations Williamstown and Geelong (see Fig. 1 and Table 1). Here, simulated amplitudes are overestimated by a factor of five (M_2) and two (K_1), respectively. Both of stations lie on the coast of Port Phillip Bay, a shallow bay isolated from the Bass Strait by two peninsulas. The eastern peninsula is long and narrow, and not resolved in the model bathymetry due to the spatial averaging performed on the source ETOPO1 dataset. As such, the tidal wave from the Bass Strait penetrates into the bay and builds up in amplitude through reflection at lateral boundaries. Excluding Williamstown and Geelong from the comparison, we obtain a root mean square (RMS) error for the constituent amplitudes of 17 cm for M_2 and 2 cm for K_1, while correlation coefficients are at 0.97 and 0.99 respectively. Estimates of the median absolute difference between model and test stations can be used to quantify possible biases in a robust way (Stammer et al., 2014); corresponding values are 8 cm for M_2 and 1 cm for K_1 irrespective of whether stations in Port Phillip Bay are included or not. Median phase differences with respect to the tide gauge estimates are 21° for M_2 and 3° for K_1. These statistics give confidence in the model's accuracy and in the assertion that areas where the disagreement between model and tide gauge data is largest are where the resolution of the model has not resolved fine-structure coastal features.

Additional comparisons with gridded M_2 data were performed using the TPXO8 inverse solution, linearly interpolated to the grid of the model domain (see http://volkov.oce.orst.edu/tides for details). The RMS difference between the model and the TPXO8 data is 7 cm for M_2, and 2 cm for K_1. The variance capture (VC) of the control was also calculated to see how well the overall character of the tidal constituents was represented (e.g., Pelling and Green, 2013):

$$\mathrm{VC} = 100\left[1 - \left(\frac{\mathrm{RMSD}}{\mathrm{S}}\right)^2\right] \tag{8}$$

where RMSD is the RMS difference between the control simulation and TPXO8, and S denotes the RMS standard deviation of the TPXO8 amplitudes. The VC is above 96% for M_2 and 97% for K_1.

For validation of the simulated M_2 changes under SLR, we followed Schindelegger et al. (2018) and condensed measured M_2 trends $(\partial H, \partial G)$ and MSL rates (∂s) to response coefficients in amplitude $(r_H = \partial H/\partial s)$ and phase $(r_G = \partial G/\partial s)$. Simulated amplitude and phase changes from the 1 m FL run at the location of 14 tide gauges were interpolated from nearest neighbor cells and also converted to ratios of r_H and r_G. Graphical comparisons in Fig. 3 indicate that the model captures the sign of the observed M_2 amplitude response in 10 out of 14 cases and reproduces large fractions of the in situ variability at approximately half of the analyzed stations (e.g., Booby Island, Brisbane, Geelong, Port Hedland, Broome). A similar figure for K_1 can be found in the supporting information. Model-to-data disparities on the northeastern seaboard (Hay Point, Gladstone) are markedly reduced in comparison to Schindelegger et al. (2018, their Fig. 7) due to the higher horizontal resolution of our setup in a region of ragged coastline features. Neither the increase of M_2 amplitudes at Townsville nor the pronounced reduction of the tide at Fort Denison (Sydney harbor) can be explained by SLR perturbations in the tidal model; both signals

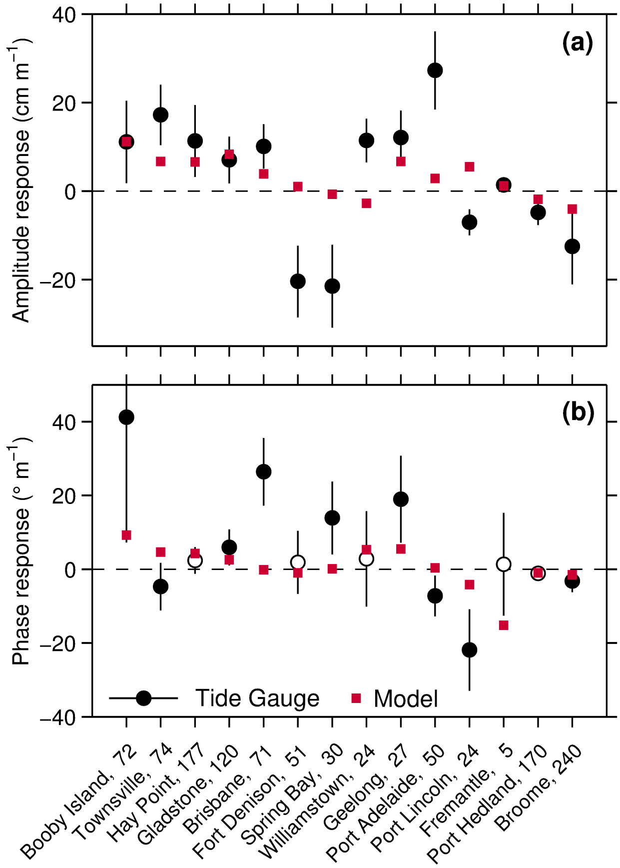

Figure 3. Observed and modeled M_2 response coefficients in (a) amplitude H and (b) phase lag G per meter of SLR. Model values (red squares) are based on the 1-m FL simulations, while tide gauge estimates at 14 out of 24 locations are shown in black. Error bars correspond to two standard deviations, propagated from the trend analyses of sea level and annual tidal estimates of M_2. Stations with insignificant phase trends (at the 95% confidence level) are shown as white markers in panel (b). Numbers at the end of the station labeling indicate mean observed M_2 amplitudes (cm)

may be the effect of periodic dredging to maintain acceptable water depths for port operations; cf. Devlin et al. (2014) for a similar analysis. The decrease of the small M_2 tide at Spring Bay, Tasmania, (20 cm m^{-1} of SLR) remains puzzling though, given that the gauge is open to the sea and unaffected by harbor activities or variable river discharge rates. Mechanisms other than SLR, such as modulation of the internal tide due to stratification changes along its path of propagation (Colosi and Munk, 2006) or variations in barotropic transports induced by thermocline deepening (Müller, 2012), need to be thoroughly addressed to complete the picture of secular changes in the surface tide. Furthermore, uncertainty in the bathymetric data due to sparsity of sounding observations may induce additional errors. Despite these limitations, our 1 m FL simulation captures good portions of the patterns of M_2 amplitude changes seen in tide gauge records around Australasia. Moreover, on time scales of centuries, water column depth changes due to SLR will outweigh tidal perturbations from other physical mechanisms. Hence, we conclude that our simulations lend themselves well for analysis of probable future tidal changes over a wider area.

3 Results

The control run exemplifies the typical tidal environment of the model domain (Figs. 1b and 6a). M_2 has large amplitudes along the north-west coast of Australia and within Joseph Bonaparte Gulf and Van Dieman Gulf. To the south-west of Australia lies a clockwise-rotating amphidrome, responsible for the westwards propagation of the tidal wave across the north Australian shelf. The interaction of this wave with the confined topography of the Arafura Sea leads to a complex tidal pattern with a notable amphidrome north of the Gulf of Carpentaria. The tide rotates anti-clockwise around New Zealand towards the east coast of Australia, where large amplitudes can be seen between Hay point and Gladstone. K_1 is dominated by a single amphidrome located within the Gulf of Carpentaria, with raised amplitudes to the north and south of this point (see the supporting information).

In general, for both constituents, the amplitude changes are not linear with respect to the imposed level of SLR (*cf.* Idier et al., 2017; Pickering et al., 2017, where tidal amplitudes across the European Shelf changed non-proportionally with SLR greater than 2 m). Relative changes are larger for lower SLR scenarios (e.g. 1 m) than for the higher SLR scenarios (e.g. 7 m). No significant differences between the FL and NFL scenarios for 1 m SLR can be seen, likely due to the fact that allowing land to flood at a 1 m SLR scenario only increased the wetted area by 12 grid cells (on our 1166 x 2000 computational grid), while at 7 m SLR 3320 new ocean grid cells were generated. Accordingly, for larger sea-level increases the differences between the Fl and NFL scenarios become more pronounced due to the increased number of flooded cells. A detailed analysis of the impact of SLR on M_2, and more peripherally K_1, is given below; the most common locations discussed are shown in Fig. 1a.

3.1 Effect of SLR on the M_2 tide

SLR brings some fairly significant changes to the M_2 tidal systems around Australia. Many of the regions which stand out as having high M_2 amplitude at present (see Fig. 1b) suffer a marked reduction in amplitude with increasing SLR (Fig 4a and c). To the north-west of Australia, amplitudes decrease in regions centered around King Sound, around Joseph Bonaparte Gulf, within Van Dieman Gulf and across the Timor Sea. The reduction in amplitude to the north-east of Van Dieman Gulf comes alongside the formation of a new amphidrome; the phase lines that run north-south in the Arafura Sea (Fig. 1b) move closer together before coalescing to form an amphidromic point. A further amphidromic point emerges in the south-east of the Gulf of Carpentaria, around the Wellesley Islands, when a virtual amphidromic point (an amphidrome over land) moves north to become real (an amphidrome over the ocean). Both these points form some time between 3 and 5 m SLR (not shown). The amphidrome that sits north of the Gulf of Carpentaria (Fig. 6a) moves northwards with SLR in both the FL and NFL scenarios, eventually becoming virtual at the higher SLR scenarios by moving over Yos Sudarso Island. This movement is therefore associated with the change in the propagation properties of the incoming tidal wave, rather than the inundation of Yos Sudarso Island which occurs at 5 m SLR and above.

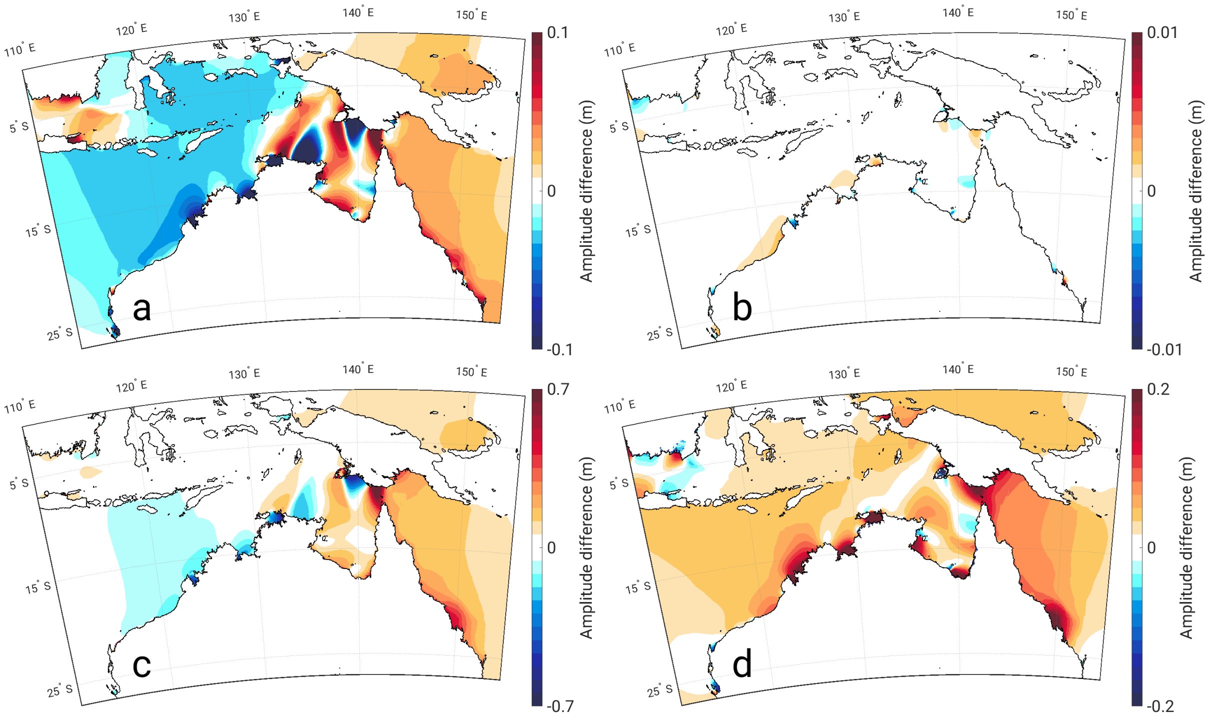

Figure 4. The difference in M_2 amplitude (m) between the FL and control simulation (i.e. FL - Control) for 1 m SLR (a) and 7 m SLR (c) alongside the difference between the NFL and FL simulations (i.e. NFL - FL) for 1 m SLR (b) and 7 m SLR (d). The scale applied to (a) and (c) is relative to the applied SLR scenario. Regions that appear blue in b) and d) are where the FL amplitude is greater than the NFL amplitude; as such coastal areas which have been flooded will appear blue.

The Torres Strait features a sharp divide between a large positive and small or weakly negative amplitude difference on its west and east sides respectively. The strait is shallow and dotted with islands, restricting the flow of the tides. Absolute amplitudes on the east side are initially elevated compared to the west (Fig. 1b) but this difference is mitigated with increasing SLR, as the larger volume of the channel allows for enhanced tidal transports across the strait (Figs. 4a and c).

In the remaining part of the domain the M_2 amplitudes around the coast of New Zealand and along the east coast of Australia, particularly between Hay Point and Gladstone (Fig. 1a, points 3 and 4), both increase with SLR. In the Bass Strait, shown in Fig. 5, the amplitude also increases along with SLR, however there is a slight drop in amplitude at 1 m SLR at the eastern entrance of the Strait and within Port Phillip Bay (the location of the Geelong and Williamstown tide gauges). These decreases quickly disappear at higher SLR. Along the south coast of Australia the amplitudes also increase with SLR, but the simulated perturbations there are generally smaller in magnitude than in the north (see also Schindelegger et al., 2018). Increased tidal amplitudes at the head and mouth of Spencer Gulf (Fig. 5a) are associated with a slight weakening of a standing wave like pattern where M_2 amplitudes increase from the sea towards inland (Fig. 1b). However, this feature does not evolve proportionally with the imposed level of SLR (see Fig. 5c for the 7 m case). To the east, in Gulf St. Vincent, there is a similar,

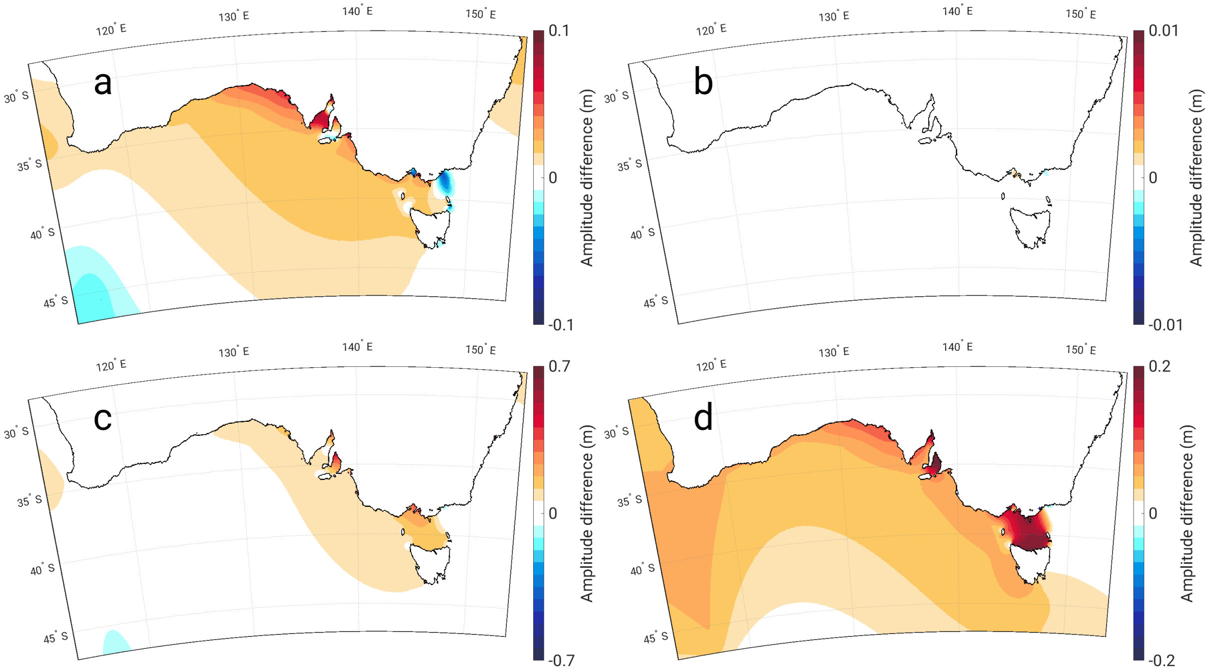

Figure 5. Same as Fig. 4 but showing the south coast of Australia.

if stronger, standing wave-like pattern (Fig. 1b). Here, the elevated amplitudes proximity to the coast increase in line with SLR (Fig. 5c). Moving further west along the south coast of Australia, the amphidromic point off the south-west coast moves southwards with increasing SLR (Fig. 6a and b), with a faster progression in the NFL than in the FL runs. Note that, almost universally across the domain, the amplitudes seen in the NFL runs are higher than those in the FL runs (Figs. 4d and 5d). It is clear that allowing flooding to occur suppresses the magnitude of any SLR effect upon tidal amplitude.

Additionally, we have repeated our control and future simulations using boundary conditions taken from TPXO8, i.e., using present day boundary conditions, instead of those from global SLR simulations. In these runs the magnitude and spatial distribution of the amplitude changes are vastly different from the results presented above. Figure 7 demonstrates, and allows for a comparison of, the pattern of amplitude changes seen for M_2 north of Australia in these runs. Especially striking is the difference in magnitude of tidal amplitude increases along the east coast of Australia. Applying present-day boundary conditions leads to a very strong underestimation of the amplitude changes in this area (the differences exceed 40 cm in some locations). Similarly pronounced is the difference on the north-west coast where the run with present day boundary conditions overestimates the amplitude decreases. In large parts of the Arafura Sea, the tidal amplitude responses are of opposite sign in response to the different boundary conditions. This is a key result and it highlights the importance of applying correct boundary condition for regional simulations which take into account the far-field change occurring outside the model domain.

Figure 8a displays the dissipation associated with the M_2 tidal constituent for the control simulation. It is evident that a majority of the energy is lost at the coast and on the shelf, especially around sharp and shallow bathymetric features. There is a

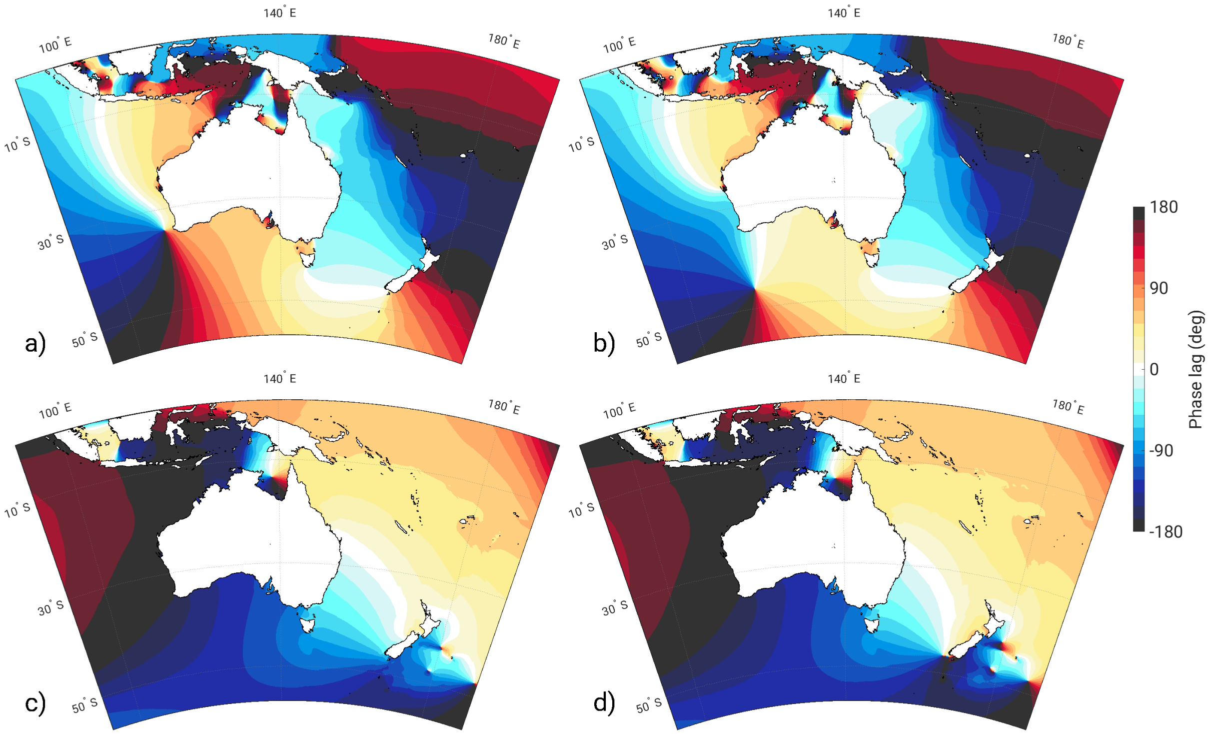

Figure 6. The constituent phase lags with respect to the Greenwich Meridian (deg) for the control (left) and 7 m SLR (right) simulations for M_2 (top) and K_1 (bottom)

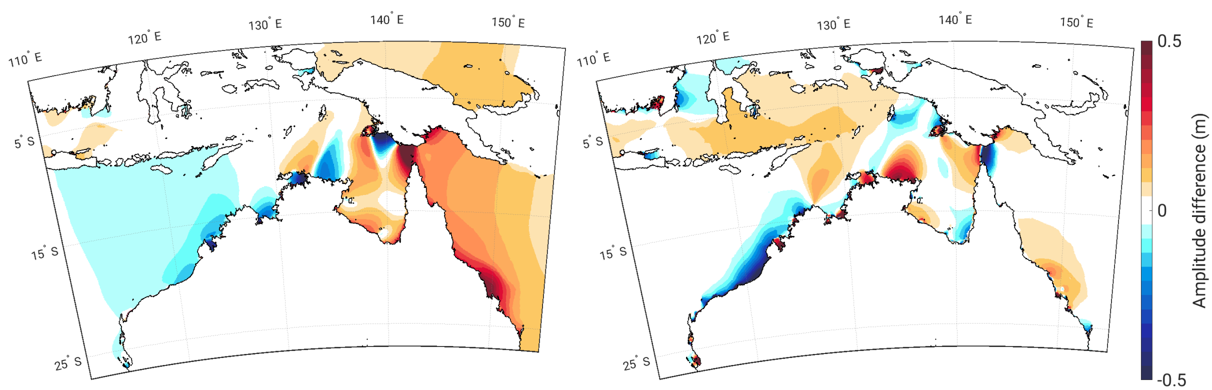

Figure 7. The difference in M_2 amplitude (m) between the FL and control simulation (i.e. FL - Control) for 7 m SLR using boundary conditions generated from a global 7 m SLR scenario (left) and using boundary conditions generated from TPXO8 (right).

remarkable reduction in dissipation along the north-west coast of Australia with SLR, matching areas with a marked decrease in tidal amplitude (Fig. 8b). There are small pockets of dissipation increases in proximity to the coast in the north-west, associated with areas of enhanced flooding. Much of the dissipation increases within the domain comes from the undersea

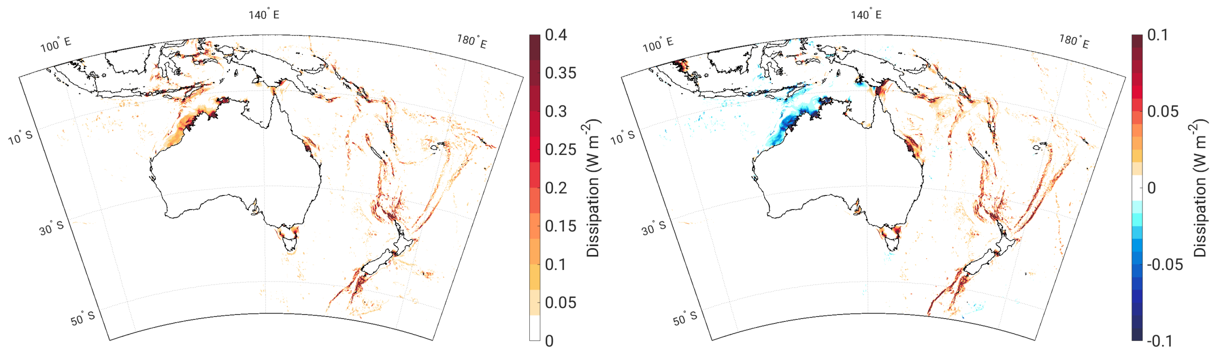

Figure 8. The dissipation (W m^{-2}) associated with the M_2 constituent across the entire model domain (left) and the difference in dissipation between the 7 m FL simulation and the control run (i.e. FL - Control, right).

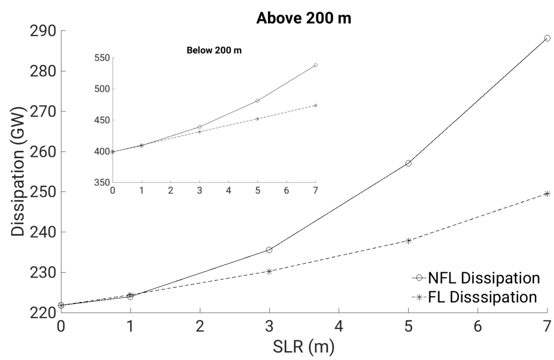

Figure 9. The dissipation totals (GW) across the model domain above and below (inset) the depth of the 200 m isobath of the control bathymetry.

ridges and trenches to the north and south of New Zealand, as well as the east side of the Torres Strait, the area between Hay Point and Gladstone on the east coast of Australia (at the southern extent of the Great Barrier Reef), and both ends of the Bass Straight. All of these areas are associated with an increase in M_2 amplitude with SLR.

The impact upon the total dissipation across the domain by allowing flooding is illustrated in Fig. 9. In both the NFL and FL runs, dissipation increases with SLR; the dissipation generated by areas with increased amplitudes outweighs the loss of dissipation in areas of decreased amplitude. With amplitudes in the NFL runs being much higher than in the FL runs the corresponding dissipation is higher, and the gap in dissipation between the NFL and FL simulations widens with increasing SLR. At 12 m SLR the NFL dissipation begins to plateau whilst the FL dissipation continues to rise. Overall, dissipation on the shelf (nominally above the 200 m isobath, accounting for approximately 7% of the water covered area of the domain) amounts to about half of the energy dissipated in deeper water.

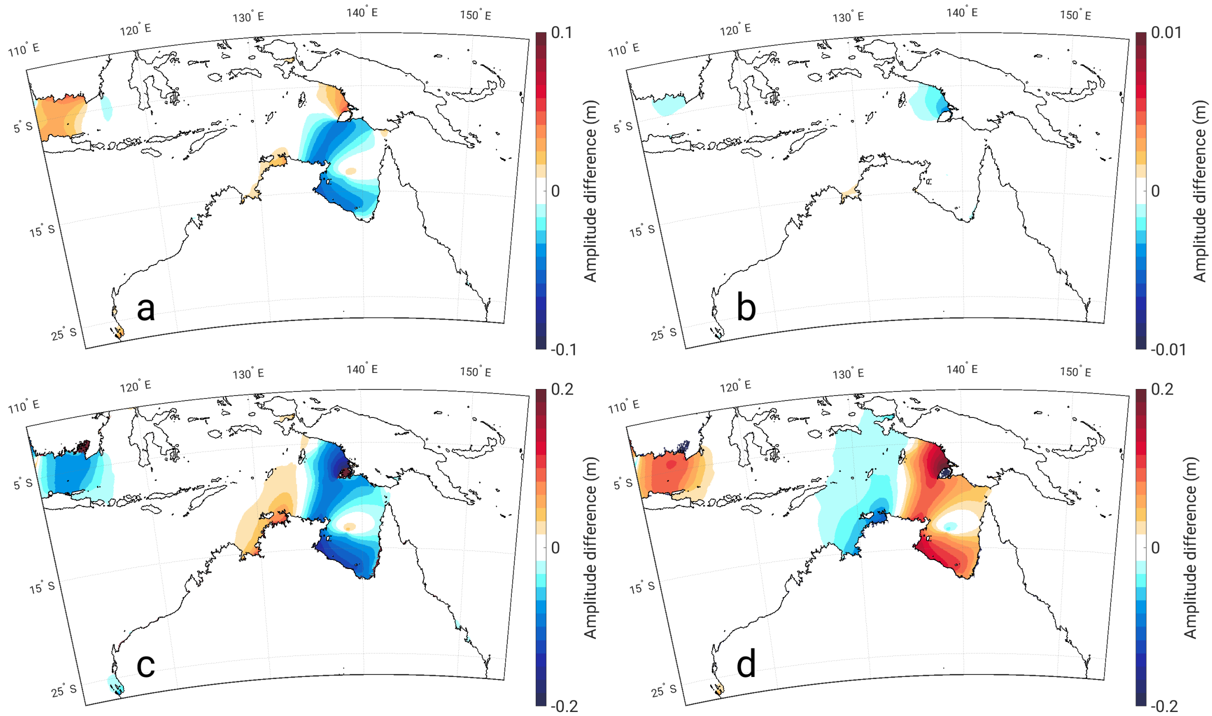

Figure 10. Same as Fig. 4 but for the K_1 constituent

3.2 Effect of SLR on the K_1 tide

The changes to K_1 are relatively small in comparison to the changes seen for the semi-diurnal constituent. The main point of interest is the amphidromic system in the Gulf of Carpentaria. Figure 10 shows an initial negative amplitude response in the north and south of the Gulf, while there are slight increases in amplitude north of Yos Sudarso Island and in the Java Sea. The position of the amphidromic system is relatively stable with SLR, as evident from the constituent phase plots in Fig. 6c and 6d, and it is evident that K_1 suffers a decrease in amplitude around the Gulf of Carpentaria with SLR. Comparing Fig. 10c and 10d, a majority of the amplitude difference occurring in the FL scenario is negated when impermeable coastlines are implemented. The dissipation for which K_1 is responsible in the domain is approximately seven times smaller than that of M_2, and therefore not discussed further.

3.3 Synthesis

One of the most striking characteristics of the response of the semi-diurnal constituents to SLR is the drop in amplitude along the north-west coast of Australia, an area where a large amount of dissipation occurs in the control. We associate this feature with the altered propagation properties of the incoming tidal wave, as the imposed sea-level change in our simulations represents a significant fraction of the average water depth across the shelf; for instance the 7 m SLR scenario increases the depth of the Gulf of Carpentaria by ∼10%. As the tidal system goes from hosting a single wave propagating across the Arafura Sea to something more complex with multiple amphidromes within the basin, the semi-diurnal resonant response on the shelf is interrupted. This dynamical change may explain the drop in amplitudes to the north-west of Australia.

4 Discussion

It has been shown here, using a validated tidal model, that the tidal characteristics around Australia are sensitive to water column depth changes due to SLR. We show significant changes in tidal amplitudes due to the SLR, with the largest change in amplitude being 15% of the SLR signal south of Papua New Guinea and north-east of Van Dieman Gulf. The model can reproduce considerable fractions of the tidal amplitude change signals seen in the tide gauge record. This is a strong indication that the observed changes in tides are, at least in part, driven by sea level changes, and adds further motivation for our investigation.

Somewhat surprisingly, the responses of the tides to SLR are very different in both their sign and spatial patterns depending on how the open boundary conditions are implemented. Furthermore, in the simulations with TPXO8 data on the open boundary, the amplitude changes along the north east coast, home to several population centers, are strongly underestimated. The take home message here is that, opposite to what has often been assumed (e.g., Pelling and Green, 2013), simulations of the effect of SLR on tides for certain regions should not use present day boundary conditions, even if the open boundary is in the far field. There are also pronounced differences between the FL and NFL simulations. Consequently, to make accurate predictions of the future tides, local coastal defence strategies need to be known, because allowing land to flood could mitigate increases in the tidal range induced by the rising sea level. If this information is not obtainable, both scenarios need to be investigated.

However, this introduces another problem: most of Australia's largest cities lie on or near the coast, and many of them are close to the areas which may experience the largest tidal changes with SLR. It thus opens for an interesting investigation to see if unpopulated areas of the coastline could be flooded to mitigate the rising sea-level in a hybrid FL-NFL scenario. Adopting a more dynamical perspective, numerical tests employing wave forcing of different periods are proposed to distinguish if the tidal response of certain areas within the domain is largely due to resonance or frictional effects (Idier et al., 2017). Additionally, an investigation into the coupling of tidal changes for expected magnitudes of SLR and storm surges (Muis et al., 2016) within the domain could provide further insight and guidance to the future planning of coastal defenses around Australia.

In conclusion, the series of simulations presented here have shown that the tidal amplitudes along the northern coast of Australia and around the Sahul shelf region are particularly sensitive to SLR. Coastal population centers such as Adelaide and Mackay are predicted to have to deal with the consequences of increased tidal amplitudes with increasing SLR. SLR appears to be moving the semi-diurnal constituents away from resonance on the shelf and only have a small impact on the diurnal constituents in the Gulf of Carpentaria. The implementation of flooding can have a significant impact on the response of the tide by locally increasing dissipation, and should be considered essential for future tidal modeling with SLR.

Acknowledgements. Financial support for this study was made available by the UK Natural Environmental Research Council (grant NE/I030224/1, awarded to J.A.M.G) and the Austrian Science Fund (FWF, through project P30097-N29 awarded to M.S.). The sea level data came from UHSLC (https://uhslc.soest.hawaii.edu/data/) and GESLA-2 (www.gesla.org). All numerical simulations were performed using HPC Wales' supercomputer facilities. Model results are available from the authors upon request.

References

ABS: Australia (AUST) 2011/2016 Census QuickStats, viewed 9 November 2018, Tech. rep., Australian Bureau of Statistics, 2016.

Allen, G. P., Salomon, J. C., Bassoullet, P., Penhoat, Y. D., and de Grandpré, C.: Effects of tides on mixing and suspended sediment transport in macrotidal estuaries, Sedimentary Geology, 26, 69–90, https://doi.org/10.1016/0037-0738(80)90006-8, 1980.

Amante, C. and Eakins, B. W.: ETOPO1 1 Arc-Minute Global Relief Model: Procedures, Data Sources and Analysis, NOAA Technical Memorandum NESDIS NGDC-24, National Geophysical Data Center, NOAA, https://doi.org/10.7289/V5C8276M, 2009.

Caldwell, P. C., Merrifield, M. A., and Thompson, P. R.: Sea level measured by tide gauges from global oceans — the Joint Archive for Sea Level holdings (NCEI Accession 0019568), NOAA National Centers for Environmental Information, Version 5.5, Dataset, https://doi.org/10.7289/V5V40S7W, 2015.

Carless, S., Green, J., Pelling, H., and Wilmes, S.-B.: Effects of future sea-level rise on tidal processes on the Patagonian Shelf, Journal of Marine Systems, 163, 113–124, https://doi.org/10.1016/j.jmarsys.2016.07.007, 2016.

Cazenave, A. and Llovel, W.: Contemporary Sea Level Rise, Annual Review of Marine Science, 2, 145–173, https://doi.org/10.1146/annurev-marine-120308-081105, 2010.

Church, J. A. and White, N. J.: Sea-Level Rise from the Late 19th to the Early 21st Century, Surveys in Geophysics, 32, 585–602, https://doi.org/10.1007/s10712-011-9119-1, 2011.

Church, J. A., Monselesan, D., Gregory, J. M., and Marzeion, B.: Evaluating the ability of process based models to project sea-level change, Environmental Research Letters, 8, 014 051, 2013.

Codiga, D. L.: Unified tidal analysis and prediction using the UTide Matlab functions, Graduate School of Oceanography, University of Rhode Island Narragansett, RI, 2011.

Colosi, J. A. and Munk, W.: Tales of the venerable Honolulu tide gauge, Journal of Physical Oceanography, 36, 967–996, https://doi.org/10.1175/JPO2876.1, 2006.

Dangendorf, S., Marcos, M., Wöppelmann, G., Conrad, C. P., Frederikse, T., and Riva, R.: Reassessment of 20th century global mean sea level rise, Proceedings of the National Academy of Sciences, https://doi.org/10.1073/pnas.1616007114, 2017.

DeConto, R. M. and Pollard, D.: Contribution of Antarctica to past and future sea-level rise, Nature, 531, 591–597, https://doi.org/10.1038/nature17145, 2016.

Devlin, A. T., Jay, D. A., Talke, S. A., and Zaron, E.: Can tidal perturbations associated with sea level variations in the western Pacific Ocean be used to understand future effects of tidal evolution?, Ocean Dynamics, 64, 1093–1120, https://doi.org/10.1007/s10236-014-0741-6, 2014.

Egbert, G. D. and Erofeeva, S. Y.: Efficient inverse modeling of barotropic ocean tides, Journal of Atmospheric and Oceanic Technology, 19, 183–204, https://doi.org/10.1175/JPO2876.1, 2002.

Egbert, G. D. and Ray, R. D.: Estimates of M_2 tidal energy dissipation from Topex/Poseidon altimeter data, Journal of Geophysical Research: Oceans, 106, 22 475–22 502, https://doi.org/10.1029/2000JC000699, 2001.

Egbert, G. D., Bills, B. G., and Ray, R. D.: Numerical modeling of the global semidiurnal tide in the present day and in the last glacial maximum, Journal of Geophysical Research: Oceans, 109, C03 003, https://doi.org/10.1029/2003JC001973, 2004.

Green, J., Huber, M., Waltham, D., Buzan, J., and Wells, M.: Explicitly modeled deep-time tidal dissipation and its implication for Lunar history, Earth and Planetary Science Letters, 461, 46–53, https://doi.org/https://doi.org/10.1016/j.epsl.2016.12.038, 2017.

Green, J. A. M.: Ocean tides and resonance, Ocean Dynamics, 60, 1243–1253, https://doi.org/10.1007/s10236-010-0331-1, 2010.

Green, J. A. M. and Huber, M.: Tidal dissipation in the early Eocene and implications for ocean mixing, Geophysical Research Letters, 40, 2707–2713, https://doi.org/10.1002/grl.50510, 2013.

Greenberg, D. A., Blanchard, W., Smith, B., and Barrow, E.: Climate change, mean sea level and high tides in the Bay of Fundy, Atmosphere-Ocean, 50, 261–276, https://doi.org/10.1080/07055900.2012.668670, 2012.

Haigh, I. D., Eliot, M., and Pattiaratchi, C.: Global influences of the 18.61 year nodal cycle and 8.85 year cycle of lunar perigee on high tidal levels, Journal of Geophysical Research: Oceans, 116, C06 025, https://doi.org/10.1029/2010JC006645, 2011.

Hay, C. C., Morrow, E., Kopp, R. E., and Mitrovica, J. X.: Probabilistic reanalysis of twentieth-century sea-level rise, Nature, 517, 481–484, https://doi.org/10.1038/nature14093, 2015.

Hendershott, M. C.: Numerical models of ocean tides, in: The Sea vol. 6, pp. 47–89, Wiley Interscience Publication, 1977.

Idier, D., Paris, F., Le Cozannet, G., Boulahya, F., and Dumas, F.: Sea-level rise impacts on the tides of the European Shelf, Continental Shelf Research, 137, 56–71, https://doi.org/10.1016/j.csr.2017.01.007, 2017.

IPCC: Climate Change 2013: The Physical Science Basis. Contribution of Working Group I to the Fifth Assessment Report of the Intergovernmental Panel on Climate Change, Cambridge University Press, Cambridge, United Kingdom and New York, NY, USA, https://doi.org/10.1017/CBO9781107415324, www.climatechange2013.org, 2013.

McInnes, K. L., Church, J., Monselesan, D., Hunter, J. R., O'Grady, J. G., Haigh, I. D., and Zhang, X.: Information for Australian impact and adaptation planning in response to sea-level rise, Australian Meteorological and Oceanographic Journal, 65, 127–149, 2015.

Muis, S., Verlaan, M., Winsemius, H. C., Aerts, J. C. J. H., and Ward, P. J.: A global reanalysis of storm surges and extreme sea levels, Nature Communications, 7, 11 969, https://doi.org/10.1038/ncomms11969, 2016.

Müller, M.: The influence of changing stratification conditions on barotropic tidal transport and its implications for seasonal and secular changes of tides, Continental Shelf Research, 47, 107–118, https://doi.org/10.1016/j.csr.2012.07.003, 2012.

Müller, M., Arbic, B. K., and Mitrovica, J. X.: Secular trends in ocean tides: Observations and model results, Journal of Geophysical Research: Oceans, 116, C05 013, https://doi.org/10.1029/2010JC006387, 2011.

Pelling, H. E. and Green, J. A. M.: Sea level rise and tidal power plants in the Gulf of Maine, Journal of Geophysical Research: Oceans, 118, 2863–2873, https://doi.org/10.1002/jgrc.20221, 2013.

Pelling, H. E., Green, J. A. M., and Ward, S. L.: Modelling tides and sea-level rise: To flood or not to flood, Ocean Modelling, 63, 21–29, https://doi.org/10.1016/j.ocemod.2012.12.004, 2013.

Pickering, M., Horsburgh, K. J., Blundell, J. R., Hirschi, J. J.-M., Nicholls, R. J., Verlaan, M., and Wells, N. C.: The impact of future sea-level rise on the global tides, Continental Shelf Research, 142, 50–68, https://doi.org/10.1016/j.csr.2017.02.004, 2017.

Pugh, D. and Woodworth, P.: Sea-Level Science: Understanding tides, surges, tsunamis and mean sea-level changes, Cambridge University Press, Cambridge, UK, 2014.

Schindelegger, M., Green, J. A. M., Wilmes, S.-B., and Haigh, I. D.: Can we model the effect of observed sea level rise on tides?, Journal of Geophysical Research: Oceans, 123, 4593–4609, https://doi.org/10.1029/2018JC013959, 2018.

Slangen, A. B. A., Katsman, C. A., van de Wal, R. S. W., Vermeersen, L. L. A., and Riva, R. E. M.: Towards regional projections of twenty-first century sea-level change based on IPCC SRES scenarios, Climate Dynamics, 38, 1191–1209, https://doi.org/10.1007/s00382-011-1057-6, 2012.

Stammer, D., Ray, R. D., Andersen, O. B., Arbic, B. K., Bosch, W., Carrère, L., Cheng, Y., Chinn, D. S., Dushaw, B. D., Egbert, G. D., Erofeeva, S. Y., Fok, H. S., Green, J. A. M., Griffiths, S., King, M. A., Lapin, V., Lemoine, F. G., Luthcke, S. B., Lyard, F., Morison, J., Müller, M., Padman, L., Richman, J. G., Shriver, J. F., Shum, C. K., Taguchi, E., and Yi, Y.: Accuracy assessment of global barotropic ocean tide models, Reviews of Geophysics, 52, 243–282, https://doi.org/10.1002/2014RG000450, 2014.

Stumpf, R. P. and Haines, J. W.: Variations in Tidal Level in the Gulf of Mexico and Implications for Tidal Wetlands, Estuarine, Coastal and Shelf Science, 46, 165–173, https://doi.org/10.1006/ecss.1997.0276, 1998.

Vellinga, P., Katsman, C., Sterl, A., Beersma, J. J., Hazeleger, W., Church, J., Kopp, R., Kroon, D., Oppenheimer, M., Plag, H. P., Rahmstorf, S., Lowe, J., Ridley, J., von Storch, H., Vaughan, D., van der Wal, R., Weisse, R., Kwadijk, J., Lammersen, R., and Marinova, N. A.: Exploring high-end climate change scenarios for flood protection of the Netherlands, Tech. rep., Royal Netherlands Meteorological Institute, 2009.

Watson, P. J.: Is There Evidence Yet of Acceleration in Mean Sea Level Rise around Mainland Australia?, Journal of Coastal Research, 27, 369–377, 2011.

Webb, D. J.: On the shelf resonances of the Gulf of Carpentaria and the Arafura Sea, Ocean Science, 8, 733–750, https://doi.org/10.5194/os-8-733-2012, 2012.

White, N. J., Haigh, I. D., Church, J. A., Koen, T., Watson, C. S., Pritchard, T. R., Watson, P. J., Burgette, R. J., McInnes, K. L., You, Z.-J., Zhang, X., and Tregoning, P.: Australian sea levels—Trends, regional variability and influencing factors, Earth-Science Reviews, 136, 155–174, https://doi.org/10.1016/j.earscirev.2014.05.011, 2014.

Wilmes, S.-B. and Green, J. A. M.: The evolution of tides and tidally driven mixing over 21,000 years, Journal of Geophysical Research: Oceans, 119, 4083–4100, https://doi.org/10.1002/2013JC009605, 2014.

Wilmes, S.-B., Green, J. A. M., Gomez, N., Rippeth, T. P., and Lau, H.: Global tidal impacts of large-scale ice sheet collapses, Journal of Geophysical Research: Oceans, 122, 8354–8370, https://doi.org/10.1002/2017JC013109, 2017.

Woodworth, P. L.: A survey of recent changes in the main components of the ocean tide, Continental Shelf Research, 30, 1680–1691, https://doi.org/10.1016/j.csr.2010.07.002, 2010.

Woodworth, P. L., Hunter, J. R., Marcos, M., Caldwell, P., Menéndez, M., and Haigh, I.: Towards a global higher-frequency sea level dataset, Geoscience Data Journal, 3, 50–59, https://doi.org/10.1002/gdj3.42, 2017.

Zaron, E. D. and Egbert, G. D.: Estimating open-ocean barotropic tidal dissipation: the Hawaiian ridge, Journal of Physical Oceanography, 36, 1019–1035, https://doi.org/10.1175/JPO2878.1, 2006.

Zhang, X., Church, J. A., Monselesan, D., and McInnes, K. L.: Sea level projections for the Australian region in the 21st century, Geophysical Research Letters, 44, 8481–8491, https://doi.org/10.1002/2017GL074176, 2017.